Supplemental Information

Liquid metal microparticles enabled low-cost, compact, and sensitive humidity sensors for *in situ* moisture monitoring

Xuanhan Chen,‡[a] Hao Lin,‡[a] Xiaoqi Gao,‡[ab] Yuguo Deng,‡[c] Xiaoqin Sun,[d] Mingyuan Sun,[e] Long Wang,[a] Liang Quan,[a] Wanlin Bao,[a] Weihua Li,[f] Lining Sun,[a] Hao Yang,*[a] Shiwu Zhang,*[e] Shi-Yang Tang,*[bg] and Xiangpeng Li*[a]

[a]College of Mechanical and Electrical Engineering, Soochow University, Suzhou, Jiangsu 215000, China

[b]School of Mechanical and Manufacturing Engineering, The University of New South Wales, Sydney, NSW 2052, Australia

[c]School of Mechatronics Engineering, Harbin Institute of Technology, Harbin, Heilongjiang 150001, China

[d]School of Automation, Northwestern Polytechnical University, Xi'an, Shaanxi 710072, China

[e]CAS Key Laboratory of Mechanical Behavior and Design of Materials, Department of Precision Machinery and Precision Instrumentation, University of Science and Technology of China, Hefei, Anhui 230026, China

[f]School of Mechanical, Materials, Mechatronic and Biomedical Engineering, University of Wollongong, Wollongong, NSW 2522, Australia

[g]School of Electronics and Computer Science, University of Southampton, SO17 1BJ, UK

*Corresponding author: yhao@suda.edu.cn (H. Yang), swzhang@ustc.edu.cn (S. Zhang), shiyang.tang2@unsw.edu.au (S.-Y. Tang), licool@suda.edu.cn (X. Li).

Experimental Section

Synthesis and characterization of Al@LM-MPs.

The synthesis procedure of the Al@LM-MPs is shown in Figure S2. 10 g eutectic Ga-indium (EGaIn: 75 wt% Ga and 25 wt% In, purity: 99.99%, Changsha SanTech Material, China) and 0.5 g aluminum foil (Al, flakes, purity: 99.99%, Suzhou UTOP Technology, China) are mixed in a beaker with the presence of NaOH solution (0.5 mol L^{-1}) for 20 mins at 60 °C in the water bath heating by a heat-collecting thermostatic stirrer. Then, NaOH is removed by an injector and wiped off with absorbent paper, leaving a thin oxide layer on the mixture of EGaIn and Al without the presence of NaOH. The mixture is sealed in a beaker with a plug and vigorously stirred by a mechanical agitator (VM-500 Pro, JOANLAB) for 15 mins at room temperature until the state of the mixture varied from liquid to solid microparticles to obtain the Al@LM-MPs.

The reaction process between a single Al@LM-MP and water is recorded by an inverted microscope (Eclipse TS100, Nikon, Japan) connected with an industrial digital camera (E3ISPM20000KPA, TIAN NUO XIANG, China).

Setup of the multivariate controllable environment simulator.

All experiments of Al@LM-MPs' heating performance and the LM^2H's laboratory tests are conducted in a multivariate controllable environment simulator which provides a confined environment with controllable oxygen content, humidity, and temperature. The environment simulator uses a glove box (VGB-3C, Changshu Tongrun Electronic Technology Co., LTD, China) as its main part to create an isolated working space. The glove box is airtight with switchable valves, helium can be introduced into the environment simulator to control the oxygen content.

In the simulator, a flow-controllable humidifier and desiccant ($CaCl_2$) are used to control the RH, which is measured by a humidity-temperature sensor (GSP-6, Elitech Technology, Inc, China) and a humidity probe (SFG309T, Xinghe Electron Co., LTD, China). Water vapor is applied through a tube until it reaches the set RH, thus we can control the RH during the entire experiment.

To precisely control the experiment environment temperature, an acrylic box (length: 20 cm, width: 15 cm, height: 15 cm) is fixed on a semi-conductor temperature controller (12 V, Zave Electron Co., LTD, China). The acrylic box is wrapped in insulation cotton to form a temperature-constant cavity. By setting the configuration of the temperature controller, the interior temperature of the cavity can be controlled from −10 to 30 °C. To introduce water vapor into the cavity, the tube is connected to the interior of the acrylic box through a hole (diameter of 30 mm) on the side. Also, an IR camera (HIKMICRO, H16) is put inside the simulator and fixed on the top of the temperature-constant cavity then it can monitor the heating temperature of the Al@LM-MPs through the hole on the cavity covered with an infrared glass. The simulator can provide a test environment with a temperature range from −10 to 30 °C and a humidity range from 20% RH to 90% RH (Figure S3 and S6).

Details of experiments about the heating performance of Al@LM-MPs.

Experiments are conducted in the multivariate controllable environment and all temperature monitoring of the Al@LM-MPs surface is accomplished with an IR camera. We keep all the Al@LM-MPs samples dehydrated; in case the sample reacts with H_2O molecules in the air to affect the accuracy. All Al@LM-MPs samples in experiments are filled in square molds with a length of 30 mm.

To test the relationship between the diameter of Al@LM-MPs and heating efficiency (Figure 3A), a scattered layer of Al@LM-MPs (LM/Al weight ratio: 20:1, diameter: 10 μm, 30 μm, 63 μm, 88 μm, and 200 μm) is transferred into the glove box with controlled humidity (RH: 30%, 60%, 90%) and monitor its surface maximum temperature synchronously. Each set of Al@LM-MPs with different diameters is tested three times.

To investigate the influence of LM/Al weight ratio on the heating performance of Al@LM-MPs, five groups of Al@LM-MPs (synthesized in LM/Al weight ratios from 100:1 to 5:1) are respectively monitored under incremental RH. Each set of Al@LM-MPs with different LM/Al weight ratios is tested three times.

Setup of the anaerobic environment and experiment details.

To create an environment with low oxygen content (%V O2 < 10%), helium is introduced into the multivariate controllable environment simulator. The content of oxygen is measured by an oxygen analyzer anchored in the simulator.

Fabrication environment of LM^2H.

The fabrication of LM^2H is conducted in the glove box to create an isolated environment. All materials needed for the LM^2H are sealed with plastic packing bags and then placed in the glove box forehead. Also, the desiccant is introduced to absorb all forms of water inside the sealed glove box and the environmental RH was monitored by the humidity-temperature sensor. The fabrication is conducted after the relative humidity in the sealed glove box reaches 5% RH.

Compensated humidity strategy.

In order to overcome the influence of different maximum heating temperature of Al@LM-MPs on the accuracy of the sensor under different environment temperatures, a humidity correction strategy is proposed. By determining the humidity compensation curve at different temperatures, the humidity display is converted to the environment temperature of 20 °C (set as the standard humidity).

Under a temperature of 0 °C, the correction curve can be calculated as:

$$y=(x+0.25)\times 100\%$$

where y is the corrected relative humidity under environment temperature of 20 °C, x is the relative humidity observed by the LM^2H under current environment temperatures.

Under an environment temperature of 10 °C, the correction curve can be calculated as:

$$y=(0.115x+0.325)\times 100\%$$

Under an environment temperature of 30 °C, the correction curve can be calculated as:

$$y=(0.106x+0.1)\times 100\%$$

For users' convenience, we created a humidity compensation table for LM^2H calibrated at 20 °C to be used in different environment temperatures of 0 °C, 10 °C, and 30 °C, as shown in Table S3.

Recycling LM from the used Al@LM-MPs.

The used Al@LM-MPs (~3 g) and NaOH solution (0.5 mol L^{-1}, 10 mL) are placed into a beaker. The mixture is stirred using a glass rod until the liquid metal is separated from the composite. Finally, the residual liquid waste is removed with a Pasteur pipette, and the recovered liquid metal is obtained (Video S9). The recycled liquid metal can be reused to produce Al@LM-MPs, and the heating performance is not influenced.

Table S1. Weight and cost of a LM^2H

Raw Materials	Mass (g)	Price (dollar)
Liquid metal (EGaIn)	1.6	0.61
Aluminum (Al)	0.08	$2e^{-4}$
Thermochromic ink	0.065	0.03
Polyolefine fiber	~ 0.04	$2.7e^{-4}$
Polylactic acid	~ 0.05	$2e^{-4}$
Cu foil	~ 0.25	0.003
Sticker with humidity calibrators	~ 0.055	0.014
Total	~ 2.1	~ 0.66

Table S2. Comparison among different kinds of humidity sensors

Type		WP[a]	RT[b] (s)	MR[c] (%RH)	Re[d] (%RH)	SW[e] (kg)	Cost[f] ($)
Electrical Sensor	Weng et al.[1]	Impedance	1.78	5-75	5	~2	~1800
	Mondal et al.[2]	Impedance	0.06	20-80	5	~2.2	~1800
	Guan et al.[3]	Impedance	25	11-95	20	~2	~1800
	Lei et al.[4]	Potentiometric	0.8	20-90	1	~2.5	~1800
	Ullah et al.[5]	Capacity	1.5	40-99	5	~3	~1800
	CHS[g]	Capacity	0.15	0-99	3	~0.6	~70
	Zhang et al.[6]	Optical	30	0-65	13	~5	~1800
	Xia et al.[7]	Optical	25	5-90	10	~3	~350
	Xuan et al.[8]	Acoustic	~300	3-70	10	~4	~1500
	Alam et al.[9]	Acoustic	35	0-99	10	~4	~1500
Passive Sensor	HH[h]	Physical	80	20-90	6	~0.1	~10
	Momtaz et al.[10]	Structural coloration	2	85-100	1.5	~0.002	~0.4
	Hou et al.[11]	FPC[i]	900	30-100	5	~0.002	~0.5
	Hu et al.[12]	Potentiometric (self-power)	1	40-90	10	~0.05	~10

Indicator card	Solomon[13]	Cobalt chloride	7200	40-70	10	~0.002	~1.5
	CCHIC[j]	Cupric chloride	7200	10/unit	10	0.009	~0.4
This work	LM^2H	Al@LM-MPs	4.17	30-90	10	0.002	0.66

[a]Working principle.

[b]Response time, data for commercial sensors are adopted from their datasheets or referred to American Military Specification MIL-I-8835A, USA, and Specification for humidity indicator card GJB2494-95, China.

[c]Measuring range.

[d]Resolution.

[e]System weight. data for commercial sensors are adopted from their datasheets, while data for non-commercial sensors are estimated based on experimental systems.

[f]Data for commercial sensors are adopted from their market price, while data for non-commercial sensors are estimated based on experimental systems.

[g]Commercial humidity sensor, TH40W, Miaoxin, China.

[h]Hair hydrometer. WS2021, Kehui, China.

[i]Fluorescent photonic crystal

[j]Commercial cobalt-free humidity indicator card, Dry&dry, USA.

Table S3. Humidity value compensation table

Environmental Temperature / Display Humidity	-10°C	0°C	10°C	30°C
35%	60%	60%	40%	30%
45%	#NA	70%	50%	40%
55%	#NA	#NA	60%	50%
65%	#NA	#NA	70%	60%
75%	#NA	#NA	80%	70%
85%	#NA	#NA	#NA	80%
95%	#NA	#NA	#NA	90%

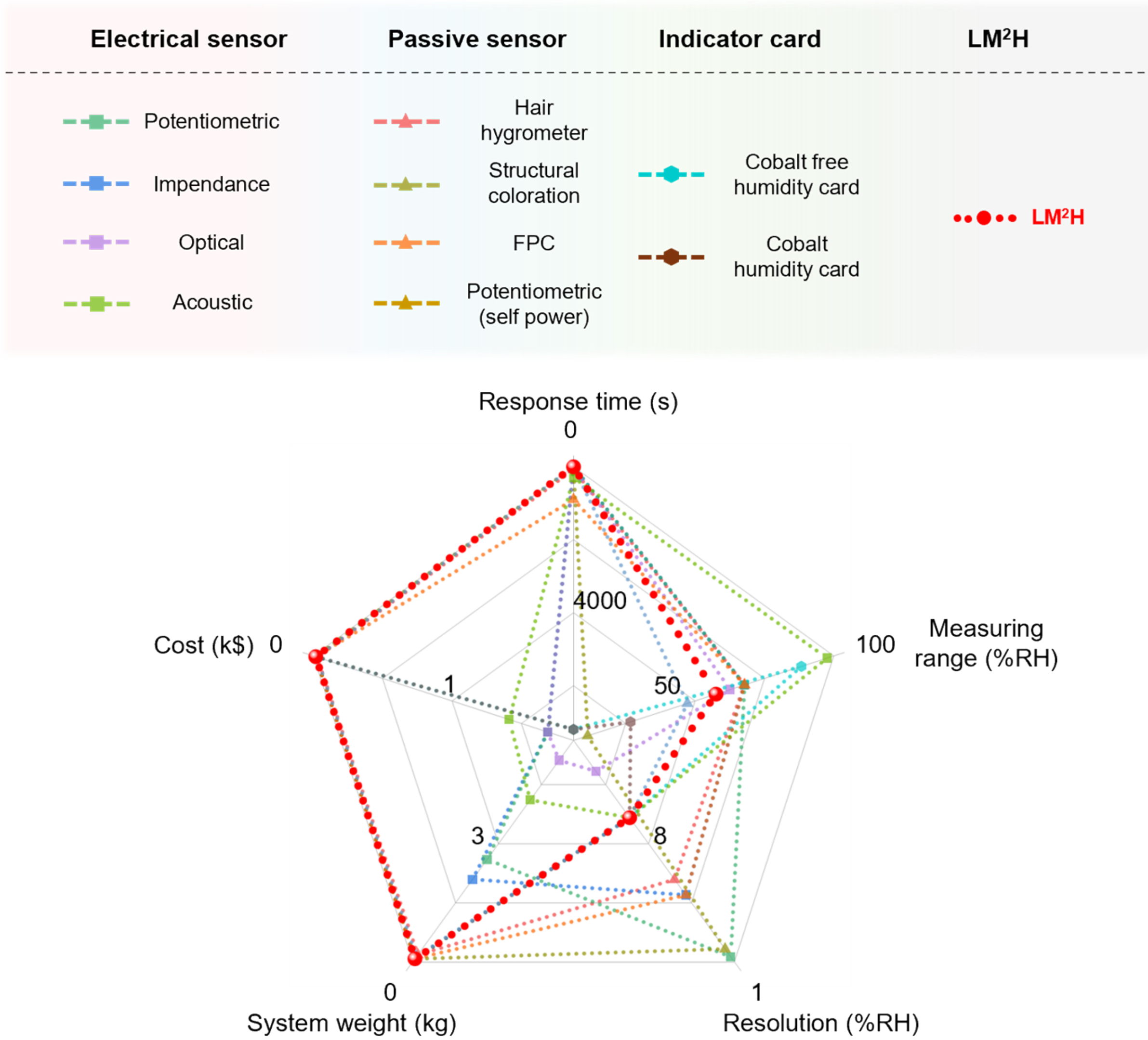

Fig. S1 LM²H compared to state-of-the-art humidity sensing technologies.

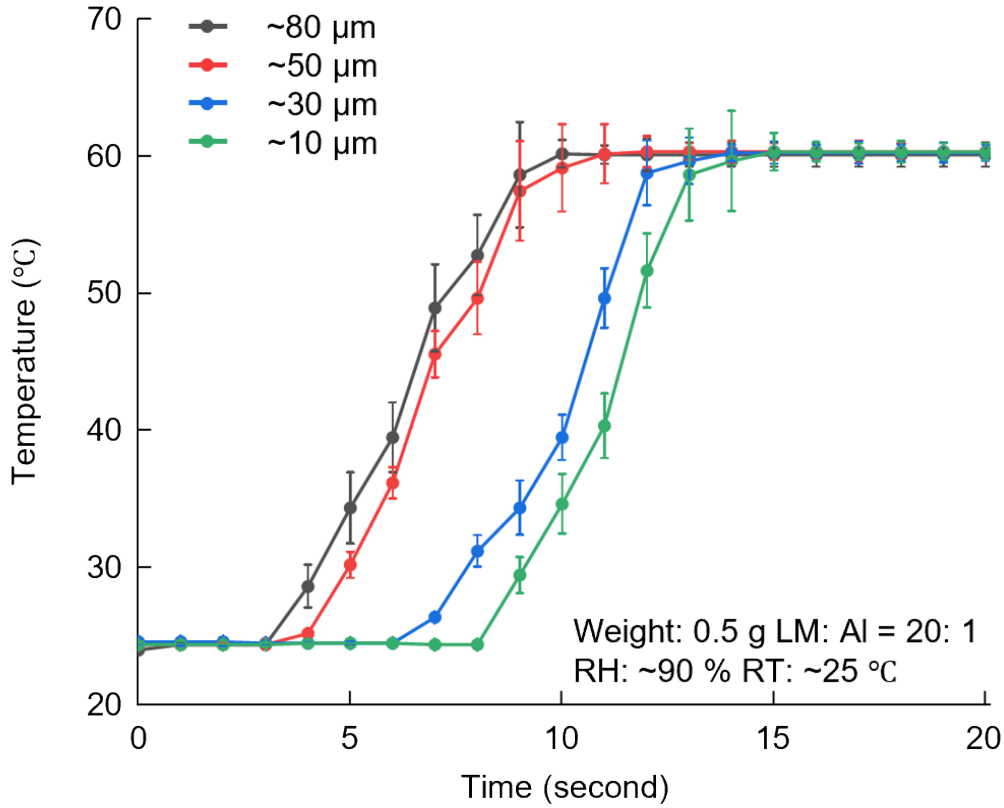

Fig. S2 The plot of heating temperature of Al@LM-MPs covered by polyester fabrics with different pore diameters under 90% RH.

Fig. S3 Size and weight of the LM^{2}H.

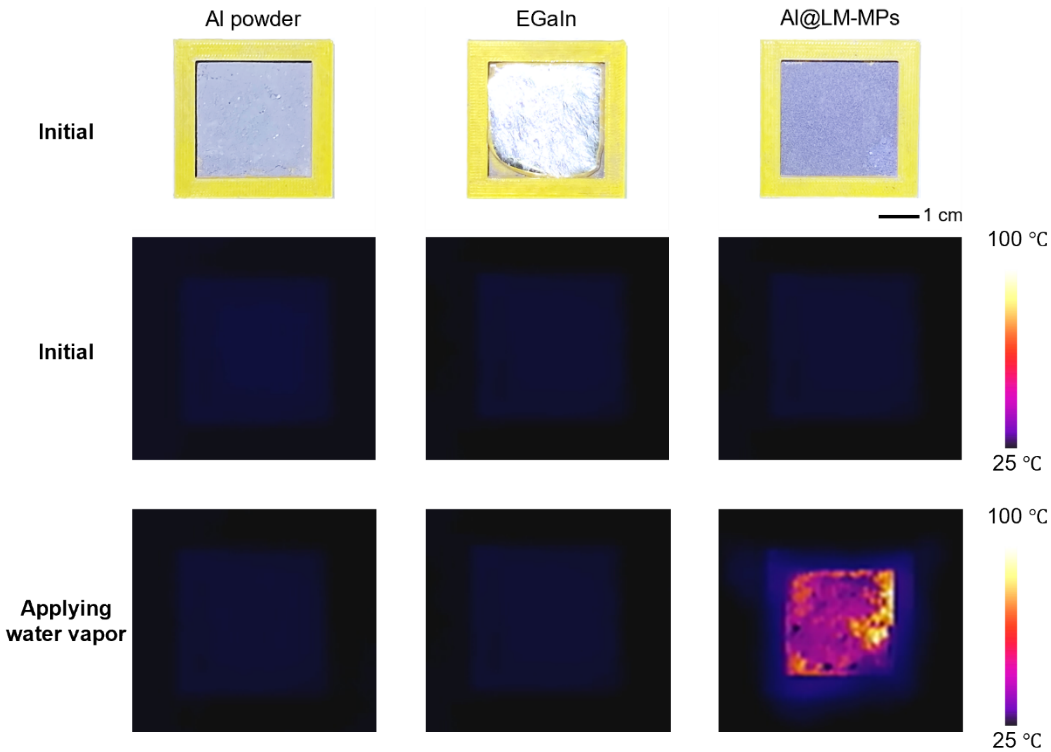

Fig. S4 The plot of heating performance of pure AI powder, pure EGaIn, Al@LM-MPs mixed with water vapor.

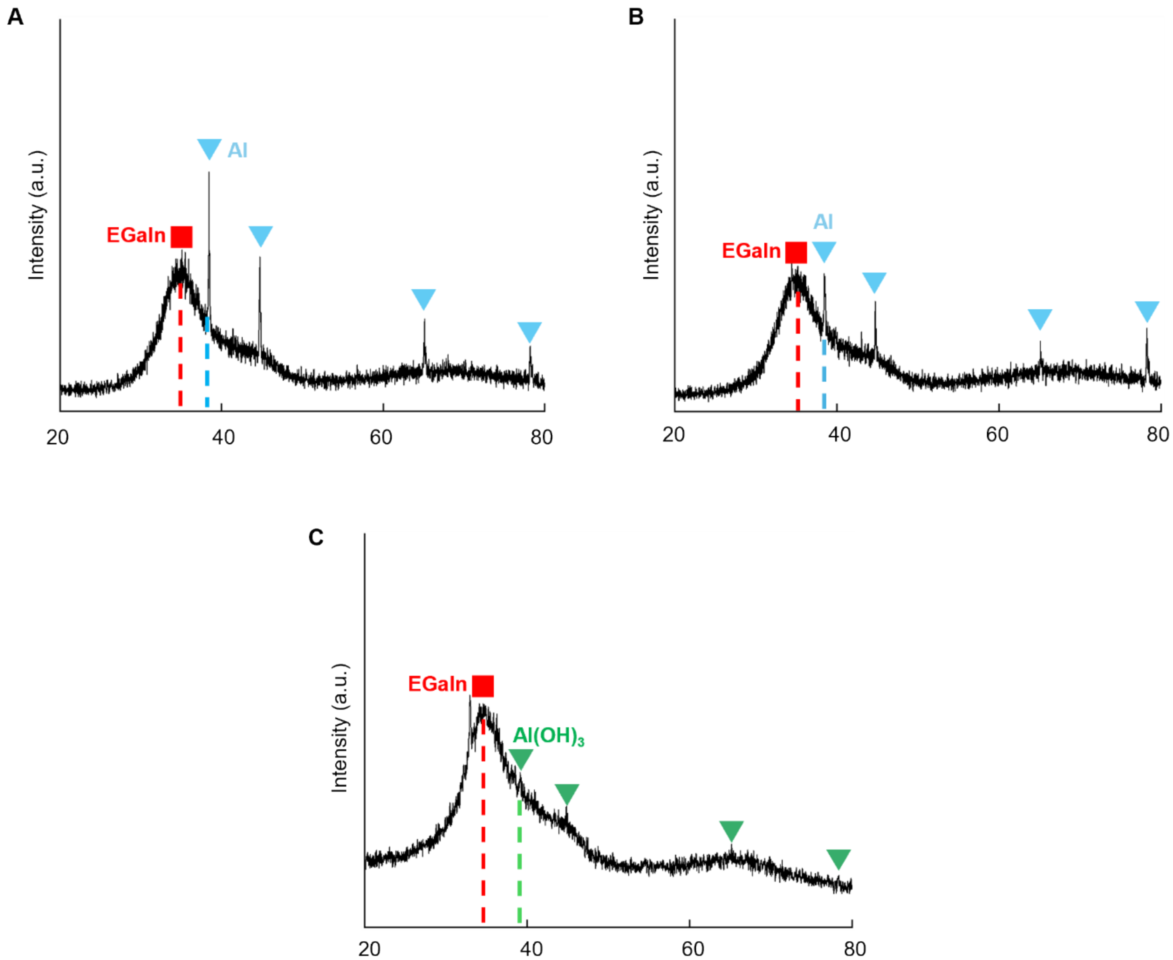

Fig. S5 XRD patterns of Al@LM-MPs in different states. (A) Fresh Al@LM-MPs. (B) Al@LM-MPs after 1h of reaction. (C) Final state of Al@LM-MPs after 10h of reaction.

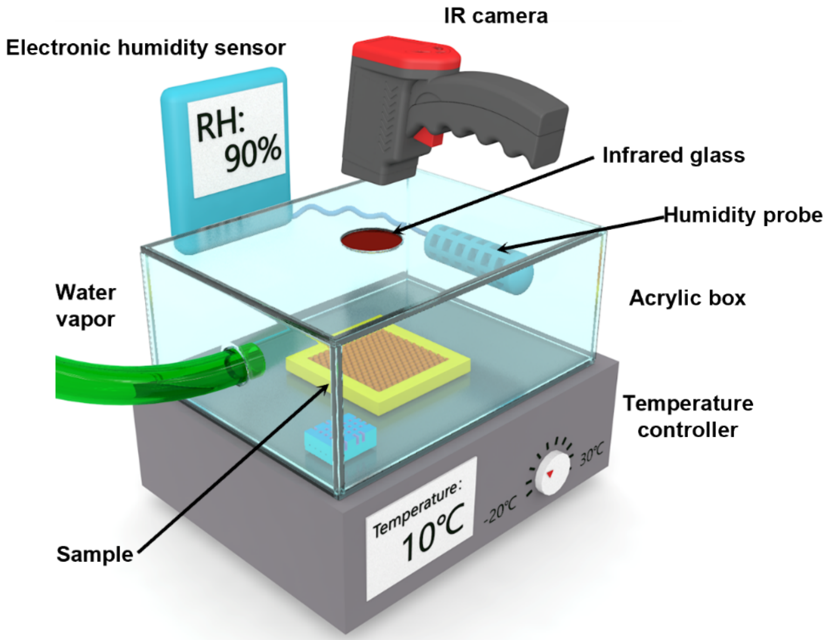

Fig. S6 Setup of the multivariate controllable environment simulator for testing heating performance of the Al@LM-MPs.

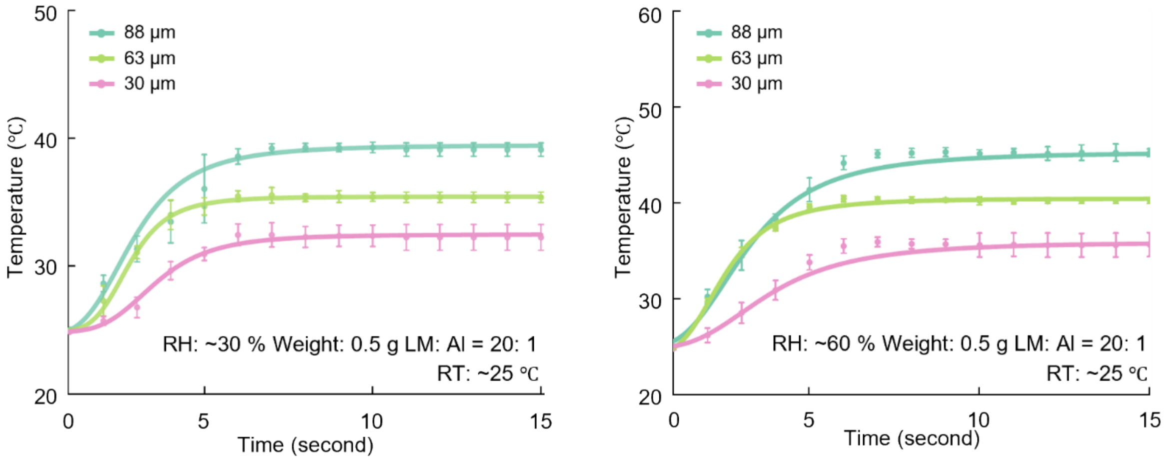

Fig. S7 Plots of heating temperature versus time with different particle sizes of Al@LM-MPs under 30% and 60% RH.

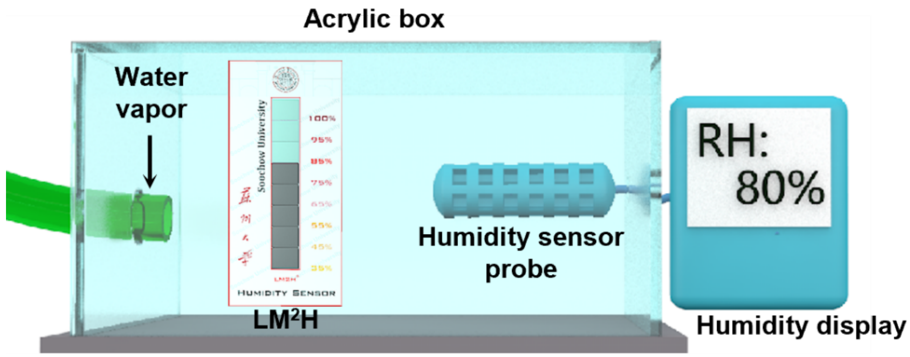

Fig. S8 Setup of the multivariate controllable environment simulator for testing humidity-sensing performance of the LM^{2}H.

Movie S1. Al@LM-MPs reacts with water under microscopic imaging.

Movie S2. Exothermic reaction of Al@LM-MPs and water under IR camera.

Movie S3. The heating performance of Al@LM-MPs sample under 90% RH.

Movie S4. Response of the LM^2H compared with a hair hygrometer.

Movie S5. LM^2H in outdoor regions.

Movie S6. LM^2H in skating rink.

Movie S7. Performance of the LM^2H and humidity indicator under severe moisture protection failure conditions by unsealing barrier bag.

Movie S8. Performance of the LM^2H and humidity indicator under slight moisture protection failure conditions by piercing barrier bag.

Movie S9. Recycle LM from the used Al@LM-MPs.

Movie S10. A comparative experiment to measure the response time of freshly prepared versus in-stock LM^2H under 90% RH.

Supporting References

1. Z. Weng, J. Qin, A. A. Umar, J. Wang, X. Zhang, H. Wang, X. Cui, X. Li, L. Zheng and Y. Zhan, Adv. Funct. Mater., 2019, **29**, 1902234.
2. S. Mondal, B. K. Min, Y. Yi and C.-G. Choi, Adv. Mater. Technol., 2022, **7**, 2100751.
3. X. Guan, Z. Hou, K, Wu, H. Zhao, S. Liu, T. Fei and T. Zhang, Sens. Actuat. B Chem., 2021, **339**, 129879.
4. D. Lei, Q. Zhang, N. Liu, T. Su, L. Wang, Z. Ren, Z. Zhang, J. Su and Y. Gao, Adv. Funct. Mater., 2022, **32**, 2107330.
5. Ullah, M. H. Zulfiqar, M. A. Khan, M. Ali, M. Zubair, M. Q. Mehmood and Y. Massoud, Sensors, 2022, **22**, 7885.
6. W. Zhang, L. Chen, Z. Yang and J. Peng, Sens. Actuat. B Chem., 2011, **155**, 226-231.
7. P. Xia, Q. Shou, T. Wang, G. Yang, H. Li, Q. Li, Y. Chen, T. Xie, J. Huang and X. Xing, Opt. Lett., 2022, **47**, 2674-2677.
8. W. Xuan, M. Cole, J. W. Gardner, S. Thomas, F.-H. Villa-López, X. Wang, S. Dong and J. Luo, J. Micromech. Microeng, 2017, **27**, 055017.
9. S. Alam, T. Islam and U. Mittal, IEEE Sens. J., 2020, **20**, 546-551.

10. M. Momtaz and J. Chen, ACS Appl. Mater. Interfaces, 2020, **12**, 54104-54116.
11. A. Hou, H. Chen, C. Zheng, K. Xie and A. Gao, ACS Nano, 2020, **14**, 7380-7388.
12. L. Hu, T. Zhong, Z. Long, S. Liang, L. Xing and X. Xue, Nanotechnology, 2023, **34**, acb94c.
13. M. E. Solomon, Ann. Appl. Biol., 1945, **32**, 75-85.